Physical Sciences

Selected Papers on Protoplanetary Disks

Ames Research Center, Moffett Field, California

Three papers present studies of thermal balances, dynamics, and electromagnetic spectra of protoplanetary disks, which comprise gas and dust orbiting young stars. One paper addresses the reprocessing, in a disk, of photons that originate in the disk itself in addition to photons that originate in the stellar object at the center. The shape of the disk is found to strongly affect the redistribution of energy. Another of the three papers reviews an increase in the optical luminosity of the young star FU Orionis. The increase began in the year 1936 and similar increases have since been observed in other stars. The paper summarizes astronomical, meteoric, and theoretical evidence that these increases are caused by increases in mass fluxes through the inner portions of the protoplanetary disks of these stars. The remaining paper presents a mathematical-modeling study of the structures of protostellar accretion disks, with emphasis on limits on disk flaring. Among the conclusions reached in the study are that (1) the radius at which a disk becomes shadowed from its central stellar object depends on radial mass flow and (2) most planet formation has occurred in environments unheated by stellar radiation.

This work was done by K. R. Bell and P. M. Cassen of **Ames Research Center***, J. T. Wasson and D. S. Woolum of the University of California, and H. H. Klahr and Th. Henning of the Max Planck Society (Jena, Germany). Further information is contained in a TSP (see page 1).*
ARC-14986

Module for Oxygenating Water Without Generating Bubbles
No bubbles were observed at any of the test flow rates.

Lyndon B. Johnson Space Center, Houston, Texas

A module that dissolves oxygen in water at concentrations approaching saturation, without generating bubbles of oxygen gas, has been developed as a prototype of improved oxygenators for water-disinfection and water-purification systems that utilize photocatalyzed redox reactions. Depending on the specific nature of a water-treatment system, it is desirable to prevent the formation of bubbles for one or more reasons: (1) Bubbles can remove some organic contaminants from the liquid phase to the gas phase, thereby introducing a gas-treatment problem that complicates the overall water-treatment problem; and/or (2) in some systems (e.g., those that must function in microgravity or in any orientation in normal Earth gravity), bubbles can interfere with the flow of the liquid phase.

The present oxygenation module (see Figure 1) is a modified version of a commercial module that contains >100 hollow polypropylene fibers with a nominal pore size of 0.05 μm and a total surface area of 0.5 m^2. The module was originally designed for oxygenation in a bioreactor, with no water flowing around or inside the tubes. The modification, made to enable the use of the module to oxygenate
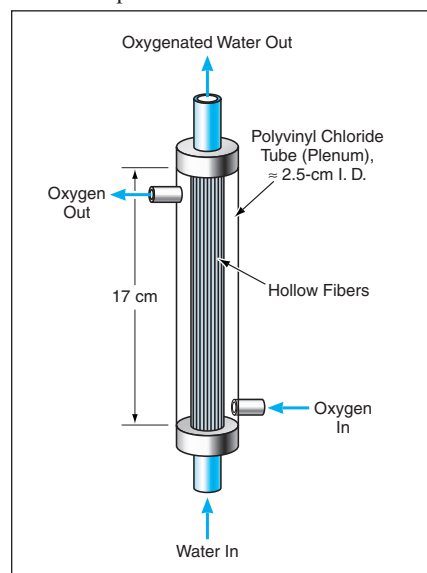

Figure 1. **Hollow, Porous Polypropylene Fibers** contain flowing water. Oxygen diffuses through the fiber walls and is dissolved in the water.
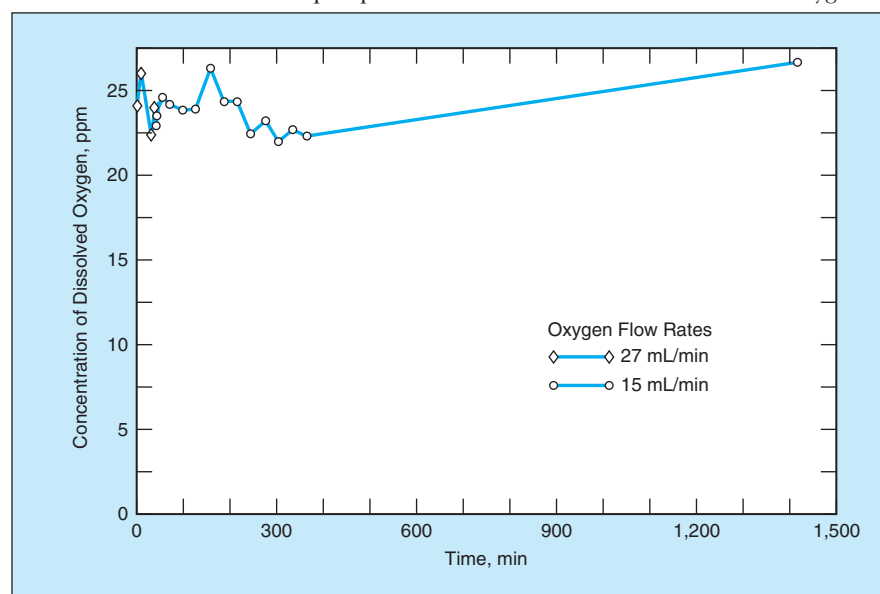

Figure 2. The **Concentration of Dissolved Oxygen** as a function of time was measured with water flowing through the module at a rate of 300 mL and with two different oxygen-flow rates.

flowing water, consisted mainly in the encapsulation of the fibers in a tube of Tygon polyvinyl chloride (PVC) with an inside diameter of 1 in. ($\approx$25 mm). In operation, water is pumped along the insides of the hollow fibers and oxygen gas is supplied to the space outside the hollow tubes inside the PVC tube.

In tests, the pressure drops of water and oxygen in the module were found to be close to zero at water-flow rates ranging up to 320 mL/min and oxygen-flow rates up to 27 mL/min. Under all test conditions, no bubbles were observed at the water outlet. In some tests, flow rates were chosen to obtain dissolved-oxygen concentrations between 25 and 31 parts per million (ppm) — approaching the saturation level of $\approx$35 ppm at a temperature of 20 °C and pressure of 1 atm ($\approx$0.1 MPa).

As one would expect, it was observed that the time needed to bring a flow of water from an initial low dissolved-oxygen concentration (e.g., 5 ppm) to a steady high dissolved-oxygen concentration at or near the saturation level depends on the rates of flow of both oxygen and water, among other things. Figure 2 shows the results of an experiment in which a greater flow of oxygen was used during the first few tens of minutes to bring the concentration up to $\approx$25 ppm, then a lesser flow was used to maintain the concentration.

Coastal Research Imaging Spectrometer

Color and temperature images yield information on contents and sources of flows.

Stennis Space Center, Mississippi

The Coastal Research Imaging Spectrometer (CRIS) is an airborne remote-sensing system designed specifically for research on the physical, chemical, and biological characteristics of coastal waters. The CRIS includes a visible-light hyperspectral imaging subsystem for measuring the color of water, which contains information on the biota, sediment, and nutrient contents of the water. The CRIS also includes an infrared imaging subsystem, which provides information on the temperature of the water. The combination of measurements enables investigation of biological effects of both natural and artificial flows of water from land into the ocean, including diffuse and point-source flows that may contain biological and/or chemical pollutants.

Temperature is an important element of such measurements because temperature contrasts can often be used to distinguish among flows from different sources: for example, a sewage outflow could manifest itself in spectral images as a local high-temperature anomaly.

Both the visible and infrared subsystems scan in "pushbroom" mode: that is, an aircraft carrying the system moves along a ground track, the system is aimed downward, and image data are acquired in across-track linear arrays of pixels. Both subsystems operate at a frame rate of 30 Hz. The infrared and visible-light optics are adjusted so that both subsystems are aimed at the same moving swath, which has across-track angular width of 15°. Data from the infrared and visible imaging subsystems are stored in the same file along with aircraft-position data acquired by a Global Positioning System receiver. The combination of the three sets of data is used to construct infrared and hyperspectral maps of scanned areas (see figure).

The visible subsystem is based on a grating spectrograph and a rapid-readout charge-coupled-device camera. Images of the swatch are acquired in 256 spectral bands at wavelengths from 400 to 800 nm. The infrared subsystem, which is sensitive in a single wavelength band of 8 to 10 µm, is based on a focal-plane array of HgCdTe photodetectors that are cooled to an operating temperature of 77 K by use of a closed-Stirling-cycle mechanical cooler.

The nonuniformities of the HgCdTe photodetector array are small enough that the raw pixel data from the infrared subsystem can be used to recognize temperature differences on the order of 1 °C. By use of a built-in blackbody calibration source that can be switched into the field of view, one can obtain bias and gain offset terms for individual pixels, making it possible to offset the effects of nonuniformities sufficiently to enable the measurement of temperature differences as small as 0.1 °C.
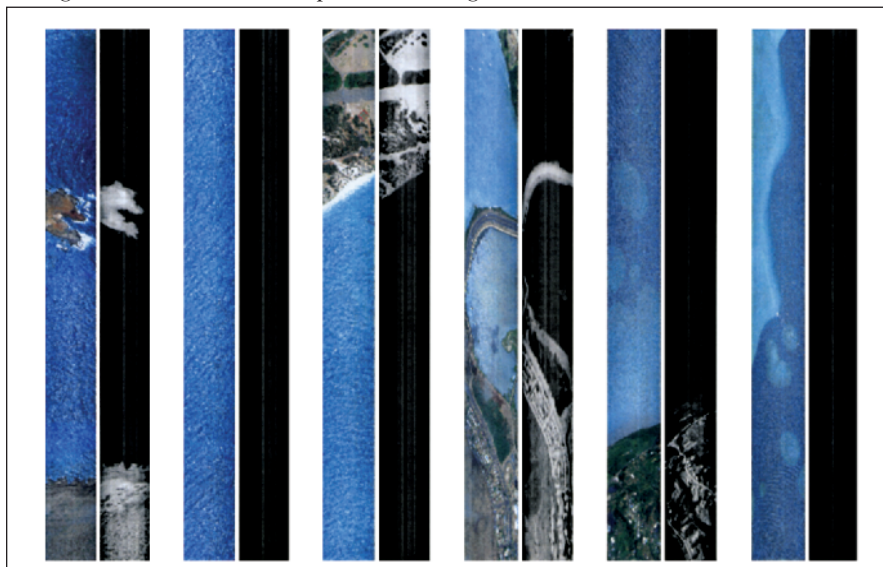
These **Color and Monochrome Images** of the same ocean areas were generated from outputs of the visible-light hyperspectral and infrared subsystem, respectively, of the CRIS during its test flight.